X-ray Thread G0.13-0.11: A Pulsar Wind Nebula?

Q. Daniel Wang, Fangjun Lu, and Cornelia C. Lang

Astronomy Department, University of Massachusetts, Amherst, MA 01003, USA

Email: wqd@astro.umass.edu, lufj@flamingo.astro.umass.edu, and clang@astro.umass.edu

ABSTRACT

We have examined *Chandra* observations of the recently discovered X-ray thread G0.13-0.11 in the Galactic center Radio Arc region. Part of the *Chandra* data was studied by Yusef-Zadeh, Law, & Wardle (2002), who reported the detection of 6.4-keV line emission in this region. We find, however, that this line emission is *not* associated with G0.13-0.11. The X-ray spectrum of G0.13-0.11 is well characterized by a simple power law with an energy slope of $1.8^{+0.7}_{-0.4}$ (90% confidence uncertainties). Similarly, the X-ray spectrum of the point-like source embedded in G0.13-0.11 has a power law energy slope of $0.9^{+0.9}_{-0.7}$. The 2 – 10 keV band luminosities of these two components are $\sim 3.2\times10^{33}$ ergs s^{-1} (G0.13-0.11) and $\sim 7.5\times10^{32}$ ergs s^{-1} (point source) at the Galactic center distance of 8 kpc. The morphological, spectral, and luminosity properties strongly indicate that G0.13-0.11 represents the leading-edge of a pulsar wind nebula, produced by a pulsar (point source) moving in a strong magnetic field environment. The main body of this pulsar wind nebula is likely traced by a bow-shaped radio feature, which is apparently bordered by G0.13-0.11 and is possibly associated with the prominent nonthermal radio filaments of the Radio Arc. We speculate that young pulsars may be responsible for various unique nonthermal filamentary radio and X-ray features observed in the Galactic center region.

Subject headings: pulsars: general — ISM: magnetic field — ISM: supernova remnant — X-rays: general — Galaxy: center

1. Introduction

The region around the dynamic center of our Galaxy is very active recently in massive star formation (e.g., Figer et al. 1999), which should have yielded various high-energy products such as supernova remnants (SNRs) and neutron stars (e.g., Morris & Serabyn 1996; Cordes & Lazio 1997; Wang, Gotthelf & Lang 2002). Young and fast-rotating neutron

stars, in particular, may be observable as pulsars, although none is yet known within 1° radius of the Galactic center (GC). Detection of radio pulsars in the GC region is difficult, because of the severe radio wave scattering by intervening interstellar ionized gas (Cordes & Lazio 1997). On the other hand, two of the polarized radio nonthermal filaments (NTFs; in the Radio Arc and G359.96+0.09) show flat or slightly rising positive spectral indices — a characteristic of Crab-like pulsar wind nebulae (PWNe; e.g., Anantharamaiah et al. 1991). *Chandra* observations have further revealed various diffuse X-ray filaments with unusually hard spectra, which are also signatures of PWNe. However, no specific link has so far been proposed between such radio/X-ray features and PWNe.

Here we report a strong candidate for a PWN that links an X-ray thread G0.13-0.11 and the prominent NTFs in the Radio Arc region (Galactic longitude $l \approx 0°.2$; Fig. 1; Yusef-Zadeh, Morris, & Chance 1984). This X-ray thread G0.13-0.11 was first apparent in the images of Yusef-Zadeh et al. (2002). The diffuse X-ray emission from the neighboring molecular cloud G0.13-0.13 (Oka et al. 2001) has been further investigated by Yusef-Zadeh, Law, & Wardle (2002). They considered the X-ray thread as part of a large-scale diffuse feature that emits the 6.4-keV fluorescent line, which results from the filling of K-shell vacancies of neutral or weakly-ionized irons (Koyama et al. 1996; Wang, Gotthelf, & Lang 2002; Wang 2002; Yusef-Zadeh, Law, & Wardle 2002). Because the prominent X-ray thread is on the side of the molecular cloud that is opposite to Sgr A*, they concluded that the 6.4-keV line emission could not represent the reflection of a possible recent radiation burst from the central massive black hole. However, our examination of related *Chandra* observations shows that the 6.4-keV line is clearly not associated with the X-ray thread G0.13-0.11, although the molecular cloud is indeed a strong 6.4-keV line emitter (e.g., Fig. 2; Wang 2002). We have conducted morphological and spectral analyses of both G0.13-0.11 and an embedded point-like source. This X-ray study, together with an investigation of the radio emission from the region, has led us to conclude that G0.13-0.11 most likely represents a PWN.

2. Observations and Astrometry Calibration

Our study used all existing *Chandra* observations of the region around G0.13-0.11; this field is shown in Fig. 1 with the important features labelled. In addition to the cycle-1 observation (50 ks; Obs. ID #945), which was used in Yusef-Zadeh et al. (2002) and Yusef-Zadeh, Law, & Wardle (2002), we included the recent GC ridge survey data (Obs. ID #2273, 2276, 2282 and 2284 — $\sim$ 11 ks each; Wang, Gotthelf, & Lang 2002) and the cycle-1 observation pointed at Sgr A* (50 ks; Obs. ID #242). The X-ray data calibration, including the CTI correction (Townsley et al. 2001), has been described by Wang, Gotthelf, & Lang

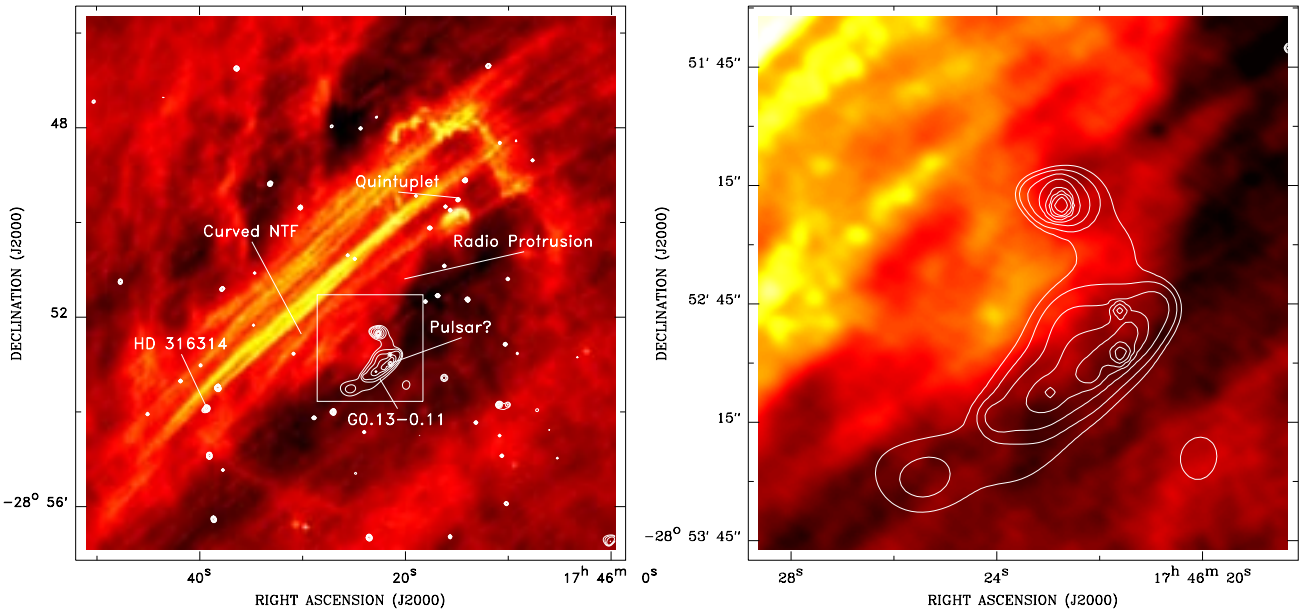

Fig. 1.— The left panel shows an overview of the region surrounding the X-ray thread G0.13-0.11: VLA 6-cm radio continuum image (§5) and the *Chandra* ACIS-I intensity contours in the 2 – 6 keV band. The square box illustrates the field of the close-up shown in the right panel. The 6-cm image is constructed from the combined CnB and DnC data and has a resolution of ∼5″. The X-ray image is adaptively smoothed, using the CIAO routine CSMOOTH with the smoothing kernel determined to achieve a signal-to-noise radio of 2.5-4. The contours are at 31, 33, 37, 45, 61, 93, 158, and 328 $\times 10^{-3}$ counts s^{-1} $arcmin^{-2}$.

(2002) and will be further detailed by Wang et al. (2002).

We searched for X-ray sources in individual observations (Wang, Gotthelf, & Lang 2002). The source position centroids are uncertain, both statistically and systematically. The statistical uncertainty depends on the count rate of a source and on the point spread function, which is a function of the off-axis angle of the source in an observation. In order to correct for the systematic pointing offset, we select sources with 2σ statistical uncertainty radii less than 1.″6.

We examined position coincidences between the X-ray sources detected in the deep observation (ID #945) and various optical/near-IR objects (e.g., ESO/ST-ECF USNO-A2.0 and 2MASS catalogs). While no coincidence was found within the 2σ statistical uncertainty radii of the X-ray source centroids, we considered objects projected within the 3″ radii of the X-ray sources. The foreground F0 star, HD316314 (B=9.94, V=9.51) stands out, which is the brightest optical object within the radii. The corresponding point-like X-ray counterpart has an ACIS-I count rate of 0.026 counts s^{-1} and a very soft spectrum. A

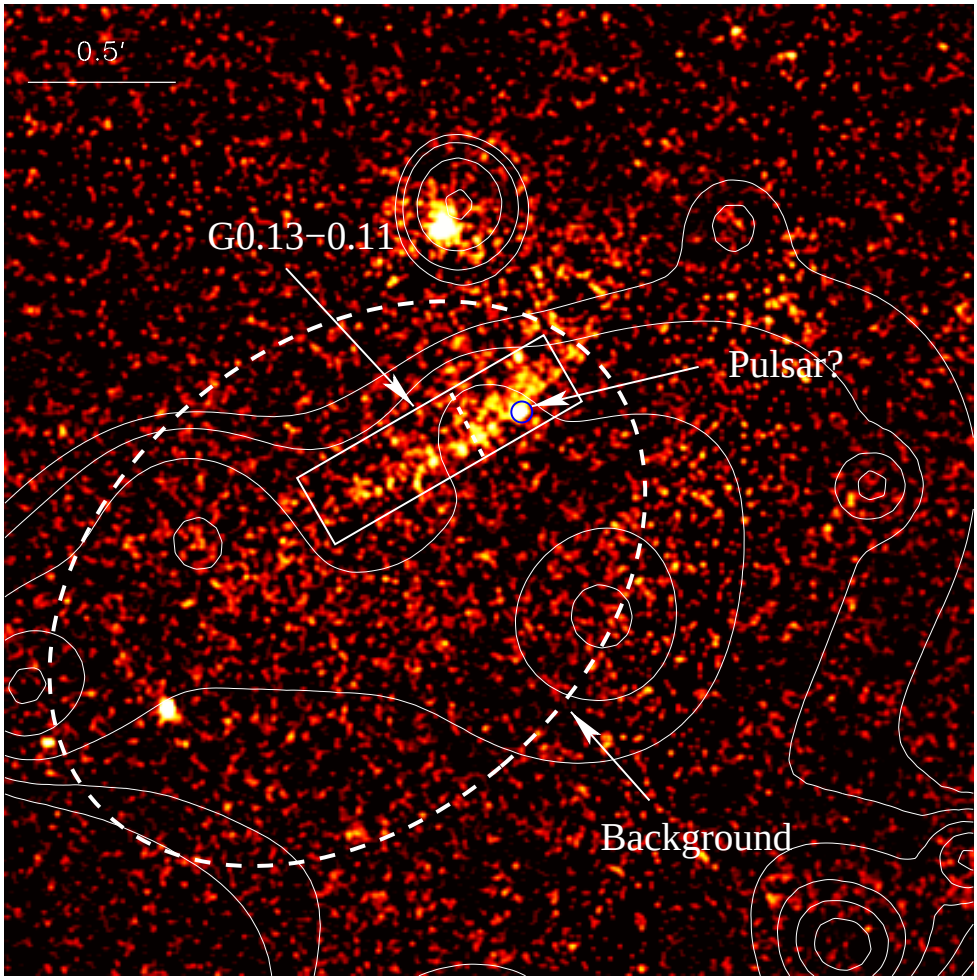

Fig. 2.— A close-up of the region around G0.13-0.11. The image represents the 2 – 6 keV intensity distribution, which has been smoothed with a Gaussian of size $\sim 1''$. The contours represent the smoothed distribution of 6.4-keV line emission at levels of 0.8, 0.9, 1.1, 1.4, 1.8, and 2.3 $\times 10^{-3}$ counts s^{-1} arcmin^{-2} (Wang 2002). Regions for the X-ray spectral analysis (§3) are also outlined.

match between the X-ray centroid and the Tycho Reference Catalog position of the star ($17^{\rm h}46^{\rm m}39\overset{\rm s}{.}075, -28^\circ 53' 51\overset{''}{.}73$; Hog et al. 1998) requires a shift of the X-ray image: $0\overset{''}{.}27$ to the west and $1\overset{''}{.}00$ to the north. Making this shift leads to the finding of several other associations between optical/near-IR objects and X-ray sources (position coincidences within the 2σ

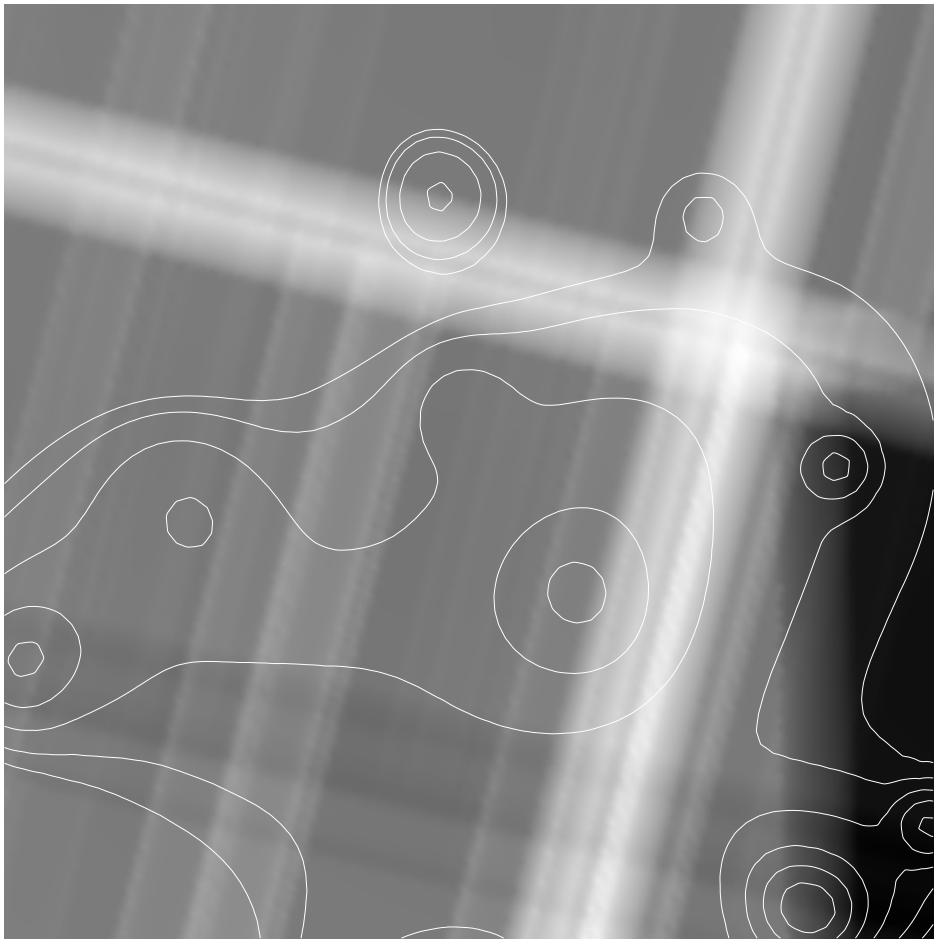

Fig. 3.— ACIS-I effective exposure map in the same field as in Fig. 2. The grey-scale represents the exposure, which ranges from 25 ks to 111 ks.

statistical uncertainty radii). The limiting R-band magnitude for the selected optical objects, for example, is 17.5. From the residual optical/X-ray position offsets of these associations, we infer that the positional inaccuracy after the correction has been made should be less than $\sim 0\farcs3$. The location of the Quintuplet cluster is also indicated in Fig. 1. This GC cluster contains numerous massive stars including the luminous Pistol Star (Figer et al. 1999). However, we detect only one possible X-ray counterpart of a cluster member. We find no counterpart for the bright X-ray source just north of G0.13-0.11, which is not considered to

be part of the X-ray thread (right panel in Fig. 1).

The focus of this paper is the X-ray thread G0.13-0.11 that borders a bow-shaped radio protrusion from the sheath of prominent NTFs and surrounds an embedded point-like X-ray source *CXOGCS J174621.5-285256* ($17^{\rm h}46^{\rm m}21\overset{\rm s}{.}51, -28^\circ52'56\overset{''}{.}5$ with an 1σ statistical uncertainty of $\sim 0\overset{''}{.}15$), marked as "pulsar?" in Figs. 1-2. We have carefully examined possible counterparts of this source in other wavelength bands. The nearest optical/near-IR object around the X-ray source is U0600-28642574 (B=17.5) at RA, Dec $= 17^h46^m21^s.81, -28^\circ52'56\overset{''}{.}0$ (J2000), about $4\overset{''}{.}0$ from the X-ray centroid. This separation far exceeds the position uncertainty of the X-ray source. Furthermore, the optical and near-IR colors of U0600-28642574 suggest that it is a nearby late-type star (later than M0) with little interstellar extinction, which is inconsistent with the large column density inferred from the X-ray spectrum (§3). We thus conclude that *CXOGCS J174621.5-285256* and U0600-28642574 do not represent the same object.

3. X-ray Properties of G0.13-0.11

Fig. 2 presents a close-up of the G0.13-0.11 field. The X-ray thread G0.13-0.13 extends $\gtrsim 40''$ to the southeast from the source *CXOGCS J174621.5-285256* and has an intrinsic width of $\sim 2''$. Fig. 3 shows potential instrumental effects in the same region as in Fig. 2. The morphology and intensity of the northwestern part of G0.13-0.11, in particular, are weakly constrained because of the poor counting statistics within a gap between CCD chips of the observation #945. The intrinsic morphology of G0.13-0.11 could be quite symmetric about the source, and thus more extensive to the northwest. Fig. 4 compares the radial surface brightness profile of the source and the telescope point spread function at the position of the observation # 945. It is clear that the source is point-like and cannot simply be a bright clump of G0.13-0.11.

Fig. 5 shows the spectra of both G0.13-0.11 and *CXOGCS J174621.5-285256*. We extracted the spectral data from the observation # 945, which was also used by Yusef-Zadeh, Law & Wardle (2002). As shown in Fig. 2, the extraction radius for *CXOGCS J174621.5-285256* is $1\overset{''}{.}5$, and a rectangular region is used for G0.13-0.11. The 6.4-keV line is completely absent in the X-ray spectra of both sources.

While the limited quality of the X-ray data alone does not allow for a serious testing of spectral models, we consider various possible origins of the X-ray emission. For example, although an one-temperature Raymond-Smith thermal plasma model gives a statistically acceptable fit, the inferred temperature has a 99% lower limit of 8 keV, which is too high to

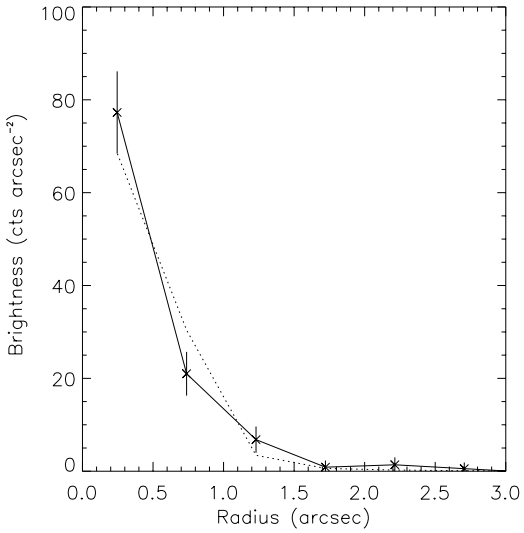

Fig. 4.— Comparison of the radial surface brightness profile (data points) of *CXOGCS J174621.5-285256* with the *Chandra* ACIS-I point-spread function (dotted line).

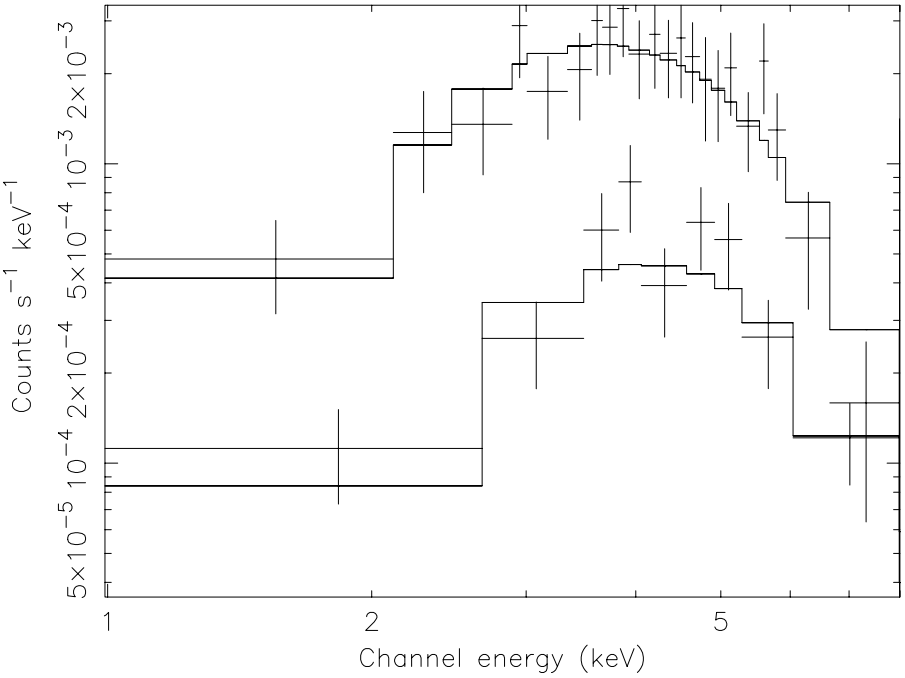

Fig. 5.— ACIS-I spectra of the X-ray thread G0.13-0.11 (above) and *CXOGCS J174621.5-285256* (below). The histograms represent the best-fit power law models of the data.

be consistent with a thermal supernova remnant interpretation. Assuming a two-temperature thermal plasma model does not solve the problem. The temperatures, if allowed to change freely, converge to the same values as high as 64 keV. If one temperature is fixed at a value of about a few keV, the other component, assuming a much higher temperature, then dominates the overall X-ray spectrum. In short, a thermal model with a temperature of a few keV has a too steep spectrum to be consistent with the data.

Furthermore, to match the observed flat spectrum with a low energy cutoff requires large amounts of absorption, which in turn demands a high emission measure. For instance, assuming that the plasma has a single temperature of 2 keV and that the depth of the X-ray-emitting region is comparable to the width ($\sim 2''$) of G0.13-0.11, we estimate the absorbing gas column density (90% confidence interval) as $5.0(3.5\text{-}6.5)\times 10^{22}$ cm^{-2} and a thermal pressure of $\sim 2 \times 10^{-7}$ dyn cm^{-2}. This pressure appears too great for the thermal gas to be confined. Even within the brightest NTFs, the dominant magnetic field pressure is $\sim 4 \times 10^{-8}$ dyn cm$^{-2} B_{\rm mG}^2$, where $B_{\rm mG}$ is the magnetic field strength in units of milli-Gauss (e.g., Yusef-Zadeh & Morris 1987). Therefore, both the high surface brightness and the flat spectral characteristics strongly suggest that the X-ray emission from G0.13-0.11 is nonthermal.

We have also tested the bremsstrahlung spectral model proposed by Valinia et al. (2000). In this case, K-shell vacancies of iron atoms are produced by collisions with low energy cosmic-ray electrons. The model is approximately a combination of a power law with an energy slope of 1.4 and a Gaussian line centered at 6.4 keV. The predicted flux ratio of the 6.4-keV line to the 2 – 10 keV continuum is about 1/26. The spectrum of G0.13-0.11, however, shows no sign of the 6.4-keV line. We can rule out the line-to-continuum flux ratio with a confidence of $\sim 3\sigma$.

A simple power law gives satisfactory fits to the X-ray spectra of both the thread G0.13-0.11 and the point-like source *CXOGCS J174621.5-285256* (Fig. 5). The best-fit energy slope is 0.9(0.2 – 1.8) for the source and 1.8(1.4 – 2.5) for the thread. The jointly-fitted X-ray-absorbing gas column density is $5.9(4.0 - 9.1) \times 10^{22}$ cm^{-2}. The column densities, if fitted separately for the two spectra, are consistent with each other, albeit with larger uncertainties. There is also statistically marginal evidence for the steepening of the power law with the distance from the source. The background-removed count flux ratio of the 4 – 8 keV band over the 2 – 4 keV band is 1.24±0.24 in the portion of the thread close to the source (the part of the rectangular box northwest to the dashed line in Fig. 2) and 0.92±0.19 in the portion away from the source (southeastern part). We infer the total absorption-corrected luminosity as $L_x \sim 4.2(3.2) \times 10^{33}$ ergs s^{-1} for the thread and $\sim 1.9(7.5) \times 10^{32}$ ergs s^{-1} for the source in the 0.1 – 2.4 keV (2 – 10 keV) band, respectively.

4. Interpretation: An X-ray-emitting Pulsar Wind Nebula?

The above morphological and spectral results place tight constraints on the nature of the point-like source *CXOGCS J174621.5-285256* and the X-ray thread G0.13-0.11. The only satisfactory interpretation that we have found is that these X-ray sources represent an isolated young pulsar and its PWN, which are likely located near the GC, consistent with the X-ray absorption measured. In this scenario, the X-ray emission from the PWN, results naturally from the synchrotron cooling of shocked pulsar wind particles (electrons and positrons). Using the empirical relation between L_x and the spin-down luminosity ($\dot{E}$) for X-ray-emitting pulsars (Becker & Trümper 1997) or for pulsar+PWN systems (Seward & Wang 1998), we estimate $\dot{E}$ for the putative pulsar to be a few times 10^{35} ergs s^{-1}, typical of an X-ray-emitting pulsar. The power law spectra we obtained for these sources are also characteristic of such a pulsar and its PWN (e.g., Gotthelf & Olbert 2002).

The X-ray morphology of our proposed pulsar/PWN system, however, is quite unique. We speculate that the slightly-curved linear morphology is due to the strong and organized interstellar magnetic field environment of the GC region (Lang et al. 1999 and references therein). Studies of the interaction between the NTFs and molecular clouds indicate a magnetic field strength of $\sim 0.1 - 1$ mG along the NTFs (e.g., Yusef-Zadeh & Morris 1987; Anantharamaiah et al. 1991; Morris & Serabyn 1996 and references therein), although the magnetic field may be weaker in the general interstellar medium. The orientation of the magnetic field (traced by radio polarization) in the vicinity of G0.13-0.11 follows the long axis of the NTFs in the Radio Arc, i.e., nearly perpendicular to the Galactic plane (Yusef-Zadeh & Morris 1987). Fig. 1 shows that the X-ray thread has a similar orientation, though not aligned with any particular NTF. This similarity indicates that the PWN may be confined by the local magnetic field.

X-ray emission traces high-energy particles in the PWN, which are most likely accelerated at the reverse shock of the pulsar wind and then move primarily along magnetic field lines. The expansion of the shocked pulsar wind (unlikely to be freely expanding) should have a velocity smaller than the thermal velocity of $c/\sqrt{3}$. The X-ray-emitting synchrotron lifetime of the particles is short, $\tau \sim (1.3 \text{ yrs})\epsilon^{-0.5}B_{\rm mG}^{-1.5}$, where ϵ is the X-ray photon energy in units of keV. From the characteristic angular scale of $40''$ from *CXOGCS J174621.5-285256* to the southeastern end of G0.13-0.11, we infer $B \lesssim 0.3$ mG. Furthermore, the balance between the ram-pressure of the pulsar wind and the magnetic field pressure gives a characteristic scale of $\sim 0\farcs04 B_{\rm mG}^{-1}[\dot{E}/(10^{35} \text{ ergs s}^{-1})]^{1/2}$ at the distance of 8 kpc. Because this scale should be smaller than the observed width ($\sim 2''$) of the X-ray thread G0.13-0.11, we have $B \gtrsim 0.02$ mG. The required magnetic field thus seems to be quite reasonable for the general interstellar medium in the GC region.

5. Radio Emission Possibly Associated with G0.13-0.11

Our interpretation of the X-ray thread G0.13-0.11 as the leading-edge of a PWN also predicts the presence of an extended radio-emitting region. The radio synchrotron lifetime of an electron is on the order of $\sim (2\times10^4$ yrs$)\nu_{\rm GHz}^{-0.5}B_{\rm mG}^{-1.5}$, about four orders of magnitude longer than the X-ray-emitting particle lifetime. Therefore, the radio emission in such a system represents the accumulation of pulsar wind material and traces the overall morphology (and "history") of the PWN.

We have obtained and reprocessed archival radio data of this region originally observed with the VLA at 20 and 6 cm in the DnC and CnB array configurations (Yusef-Zadeh et al. 1984, Yusef-Zadeh & Morris 1987) in order to compare these images to the distribution of X-ray emission and to study the spectral properties of the radio emission.

5.1. Radio Morphological Properties

An examination of the radio images shows no counterpart of the X-ray source *CXOGCS J174621.5-285256*. This is not a surprise even if the source is a young pulsar. The pulsed radio emission may be beamed away from us, or the heavy interstellar scattering may have significantly diffused the emission (Cordes & Lazio 1997).

Fig. 1 shows that the curvature of the X-ray thread G0.13-0.11 closely corresponds to the edge of a protrusion of diffuse radio emission from the southwestern edge of the prominent Radio Arc NTFs. This combination of the features suggests that our proposed PWN is produced by a pulsar moving in a strong and organized magnetic field environment. Morphologically, G0.13-0.11 differs from the Crab Nebula, in which its corresponding pulsar is deeply embedded. Instead, G0.13-0.11 shows similarities to ram-pressure confined PWNe, such as the Duck/PSR1757-24 (Thorsett et al. 2002) and LMC SNR N157B/PSR J0537-6910 (Wang et al. 2001), both of which show offsets of X-ray-emitting pulsars from radio peaks. In these latter systems, the X-ray emission arises from freshly shocked pulsar winds (thus from regions close to the pulsars) whereas radio emission arises from particles swept up (into a "trail") by the ram-pressure over the lifetime of the nebula. However, in the case of G0.13-0.11, the magnetic field likely plays a dominant role in confining and transporting shocked pulsar wind particles. As a result, a moving pulsar would leave a PWN (a bow-shaped trail of shocked wind particles) that expands primarily along the direction of magnetic field lines.

The morphological properties of the protrusion, the NTFs, and G0.13-0.11 together suggest a likely trajectory of the pulsar from the northeast to the present position. In this scenario, the synchrotron-emitting relativistic particles from the passing pulsar would cause

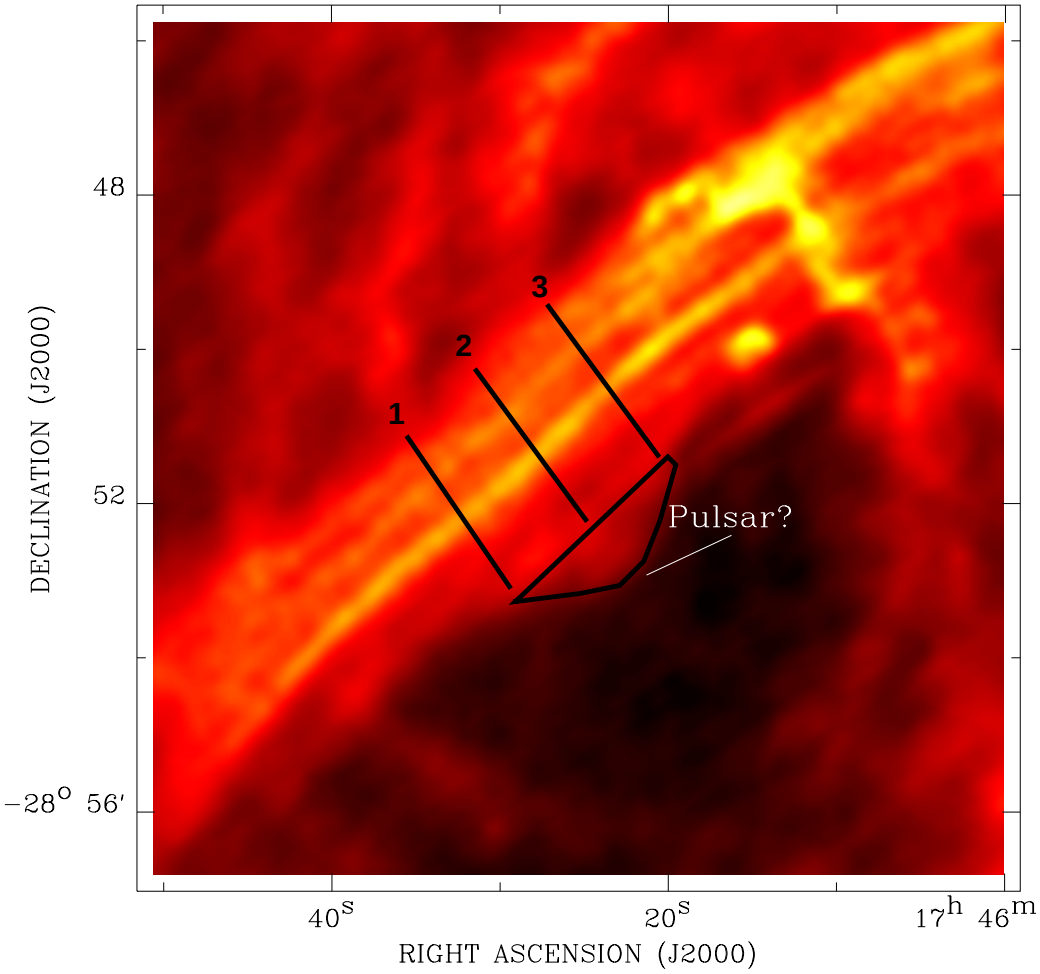

Fig. 6.— 20-cm radio continuum image of the Radio Arc region, labelled with the three cross-cuts, along which the distribution of the 20/6-cm spectral index was sampled and is shown in Fig. 7. The protrusion of diffuse radio emission directly adjacent to G0.13-0.11 is also outlined, for which an integrated 20/6-cm spectral index of α=+0.3 is calculated.

the NTFs in the Radio Arc to be illuminated. The NTF (marked as "curved NTF" in Fig. 1) that apparently most adjacent to G0.13-0.11 also shows more curvature than any of the other NTFs in the Radio Arc. The curvature of the NTFs and G0.13-0.11 may be a result of the balance between the magnetic field tension and the thermal pressure of the PWN. For the pulsar to cross the Radio Arc NTFs and the protrusion ($\sim 4'$ or 10 pc at the GC) requires $\sim 10^5$ years$(v_p/100$ km s$^{-1})^{-1}$, where v_p is the pulsar proper motion speed. Interestingly, this time is consistent with the spin-down age ($10^4 - 10^6$ years) of the pulsar expected from the observed X-ray luminosity (Becker & Trümper 1997), and may be compared to the radio synchrotron lifetime of the particles.

5.2. Radio Spectral Index

We have examined the radio spectral index in the NTFs and in the protrusion of radio emission just below the NTFs (Fig. 6). We have obtained comparable spatial resolutions ($\sim 10''$) by using the 20-cm CnB array data and the 6-cm DnC data. One concern, of course, is that the lack of total radio power in these interferometric observations may affect the absolute measurement of the spectral index. The globally averaged 20/6-cm spectral index over a circular region of $2'$ radius centered at RA, Dec (J2000) = $17^h46^m30^s, -28°51'30''$. gives a value of $\alpha\sim+0.1$ (where $S_\nu \propto \nu^\alpha$). This value is consistent with the average spectral index ($\alpha\sim+0.2\pm0.1$) measured by Reich et al. (1988) for the Radio Arc, using single-dish data. Using well-matched interferometric data therefore does not seem to significantly bias the spectral index measurement.

While the nature of the flat or slightly positive spectral index remains unclear, we speculate that the radio-emitting particles in the Radio Arc NTFs are not accelerated by shocks, which would yield a steep (negative index) synchrotron spectrum. In our interpretation, the particles represent the thermalized pulsar wind. Because the wind is believed to be ultra-relativistic and to be thermalized at the reverse shock, no acceleration is required for radio synchrotron particles. The thermalization alone would result in a Maxwellian particle energy distribution. The particles on the lower energy part of this distribution could give rise to a positive spectral index of the radio synchrotron emission. This interpretation is similar to the idea that the positive spectral index could be a result of the synchrotron emission from particles of a mono-energetic distribution (e.g., Reich et al. 1988). In contrast, X-ray-emitting synchrotron particles, which should be on the higher energy side of the Maxwellian distribution, require acceleration in the PWN, most likely at the reverse shock.

We may further expect to detect the aging of the radio-emitting particles in the PWN as a function of the distance from the pulsar. In the protrusion of diffuse radio emission directly

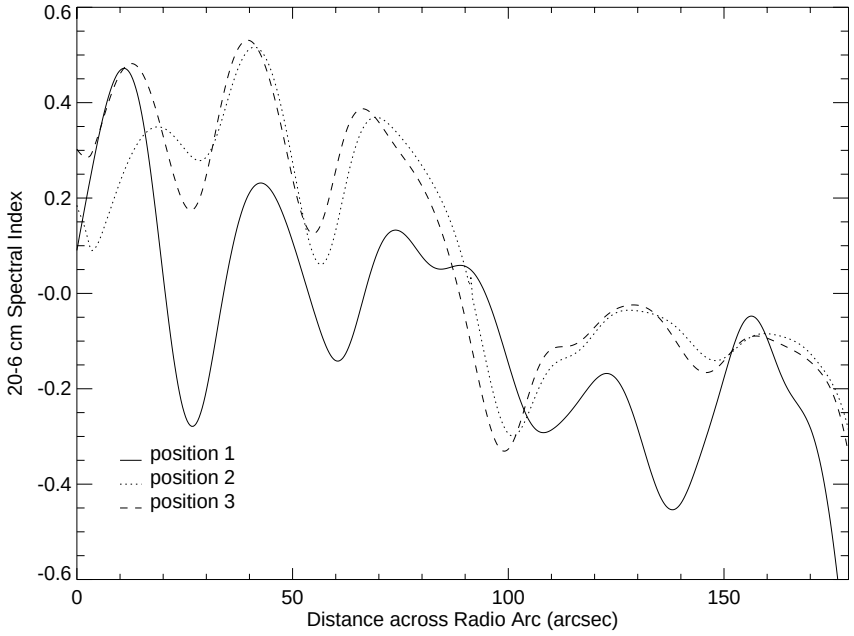

Fig. 7.— Distribution of spectral index for the three cross-cuts of the Radio Arc; sampled from the southwest to the northeast. The peaks represent the emission from the NTFs of the Radio Arc, whereas the valleys represent the weaker, diffuse component of radio emission present between the NTFs.

adjacent to G0.13-0.11 (Fig. 6), the limited signal-to-noise ratio of the radio data allows for only an estimate of the integrated spectral index of $\alpha \sim +0.3$. However, across the Radio Arc, we investigated the distribution of spectral index (Figs. 6-7). Along all three cross-cuts, the spectral indices of the NTFs have an average value of $\sim +0.4$ at the southwestern edge of the Radio Arc, and steepen to an average value of $\sim$ -0.1 in the northeastern (i.e. toward the numbers labelled 1-3) region. This spectral index steepening is consistent with our interpretation that the particles are being supplied by the pulsar along its northeast-to-southwest trajectory.

6. Conclusions

We have studied the X-ray thread G0.13-0.11 and the embedded point-like X-ray source *CXOGCS J174621.5-285256* as well as the adjacent nonthermal radio emission in the Radio Arc region. The morphological and spectral properties of these features appear to be consistent with our PWN interpretation. We hope that this study will stimulate observational and theoretical studies to further explore the connection between pulsars and various nonthermal features observed in the unique GC environment. The ultimate confirmation of the PWN interpretation requires the detection of the pulsed signal from the putative pulsar, which could be achieved with future radio and/or X-ray observations with fast timing capabilities.

We thank the referee B. Aschenbach for valuable comments that helped to improve the presentation of the work, which was supported by the SAO grant G01-2150A.

REFERENCES

Anantharamaiah, K. R., Pedlar, A., Ekers, R. D., & Goss, W. M. 1991, MNRAS, 249, 262

Baganoff, F., et al. 2001, Nature, 413, 45

Becker, W., & Trümper, J. 1997, A&A, 326, 682

Cordes, J. M., & Lazio, T. J. W. 1997, ApJ, 475, 557

Figer, D., et al. 1999, ApJ, 525, 750

Gotthelf, E.V., & Olbert, C.M., in *Neutron Stars in Supernova Remnants*, Slane, P. & Gaensler, B., eds. (San Fransisco: ASP), 171

Hog, E., et al. 1998, A&A, 335, 65

Koyama, K., et al. 1996, PASJ, 48, 249

Lang, C., Morris, M., & Echevarria, L. 1999, ApJ, 526, 727

Morris, M., & Serabyn, E. 1996, ARA&A, 34, 645

Reich, W., Sofue, Y., Wielebinski, R. & Seiradakis, J. 1988, A&A, 191, 303

Seward, F. D., & Wang, Z. R. 1998, ApJ, 332, 199

Thorsett, S. E., et al. 2002, astro-ph/0206034

Townsley, L. K., Broos, P. S., Garmire, G., & Nousek, J. 2001, ApJL, 534, 139

Valinia, A., et al. 2000, ApJ, 543, 733

Wang, Q. D., Gotthelf, E. V., Chu, Y.-H., & Dickel, J. R. 2001, ApJ, 559, 275

Wang, Q. D., Gotthelf, E. V., & Lang, C. 2002, Nature, 415, 148

Wang, Q. D. 2002, in The New Vision of the X-ray Universe in the XMM-Newton and Chandra Era, in press

Wang, Q. D. et al., in preparation.

Yusef-Zadeh, F., Morris, M., & Chance, D. 1984, Nature, 310, 557

Yusef-Zadeh, F. & Morris, M. 1987, ApJ, 322, 721

Yusef-Zadeh, F., Law, C., Wardle, M., Wang, Q. D., Fruscione, A., Lang, C., & Cotera, A. 2002, ApJ, 570, 665

Yusef-Zadeh, F., Law, C., & Wardle, M. 2002, ApJL, 568, 121

AAS LaTeX macros v5.0.